



Clouds drive differences in future surface melt over the Antarctic ice shelves

Christoph Kittel¹, Charles Amory², Stefan Hofer³, Cécile Agosta⁴, Nicolas C. Jourdain², Ella Gilbert⁵, Louis Le Toumelin⁶, Hubert Gallée², and Xavier Fettweis¹

¹Department of Geography, UR SPHERES, University of Liège, Belgium

²Univ. Grenoble Alpes/CNRS/IRD/G-INP, IGE, Grenoble, France

³Department of Geosciences, University of Oslo, Oslo, Norway

⁴Laboratoire des Sciences du Climat et de l'Environnement, LSCE-IPSL, CEA-CNRS-UVSQ, Université Paris-Saclay, Gif-sur-Yvette, France

⁵Department of Meteorology, University of Reading, Whiteknights Rd, Reading, United Kingdom

⁶Univ. Grenoble Alpes, Université de Toulouse, Météo-France, CNRS, CNRM, Centre d'Études de la Neige, Grenoble, France

Correspondence: Christoph Kittel (ckittel@uliege.be)

Abstract. Recent warm atmospheric conditions have damaged the ice shelves of the Antarctic Peninsula through surface melt and hydrofracturing, and could potentially initiate future collapse of other Antarctic ice shelves. However, model projections with similar greenhouse gas scenarios suggest large differences in cumulative 21st century surface melting. So far it remains unclear whether these differences are due to variations in warming rates in individual models, or whether local surface energy budget feedbacks could also play a notable role. Here we use the polar-oriented regional climate model MAR to study the physical mechanisms that will control future surface melt over the Antarctic ice shelves in high-emission scenarios RCP8.5 and SSP585. We show that clouds enhance future surface melt by increasing the atmospheric emissivity and longwave radiation towards the surface. Furthermore, we highlight that differences in meltwater production for the same climate warming rate depend on cloud properties and particularly cloud phase. Clouds containing a larger amount of liquid water lead to stronger melt, subsequently favouring the absorption of solar radiation due to the snow-melt-albedo feedback. By increasing melt differences over the ice shelves in the next decades, liquid-containing clouds could be a major source of uncertainties related to the future Antarctic contribution to sea level rise.

1 Introduction

Clouds are key drivers of the surface energy budget (SEB) of snow and ice. They can have opposing effects by reflecting solar (shortwave) radiation towards space and by re-emitting trapped energy through thermal (longwave) radiation towards the surface. The net cloud radiative effect - the balance between these opposite contributions - is notably determined by the surface albedo (Bintanja and van den Broeke, 1996; Hofer et al., 2017), and cloud properties, i.e their temperature (Stephens, 1984), structure (Barrett et al., 2017; Gilbert et al., 2020), and water phase (ice or liquid) (Lachlan-Cope, 2010; Hines et al., 2019; Gilbert et al., 2020). The absorption and reflection properties of clouds depend on the cloud optical depth (COD), which



20 are partly linked to their liquid water content (Stephens, 1984; Zhang et al., 1996). Liquid-containing clouds, including both liquid-only and mixed-phase clouds, have a stronger effect on the COD and therefore on the SEB than ice clouds (Bennartz et al., 2013; Gorodetskaya et al., 2015; Hofer et al., 2019).

Clouds currently warm the Antarctic Ice Sheet (AIS) surface (Pavolonis and Key, 2003; Van Den Broeke et al., 2006). While the highly-reflective snow already prevents significant absorption of solar downwelling radiation (SWD) in summer, clouds act
25 as another source of incoming energy in the infrared spectrum, which can heat and melt snow (Bintanja and van den Broeke, 1996; Van Den Broeke et al., 2006). Abundant liquid-containing clouds associated with warm and moist air advection are responsible for intense melt events due to enhanced downwelling longwave fluxes (LWD) (Nicolas et al., 2017; Scott et al., 2019; Wille et al., 2019; Ghiz et al., 2021). These liquid-containing clouds can also become a significant source of incoming energy in winter and trigger surface melt even outside of the usual summer melt season (Kuipers Munneke et al., 2018; Wille
30 et al., 2019).

Surface melting in Antarctica is currently predominantly limited to Antarctic ice shelves (Trusel et al., 2013; Van Wessem et al., 2018; Agosta et al., 2019), the floating extensions of the grounded ice sheet. Surface melt can damage the ice shelves (Lhermitte et al., 2020), potentially initiate their collapse (van den Broeke, 2005) and increase the Antarctic contribution to sea level rise (SLR) through a speed-up in glacier flow (Scambos et al., 2014). Little is known about how cloud-related uncertainties
35 will influence the future climate and surface mass balance projections over the Antarctic ice shelves.

Quantifying the influence of clouds on the SEB remains challenging over bright surfaces in high latitudes. This is particularly true over the AIS where observations are scarce and expensive to maintain (Bromwich et al., 2012; Boucher et al., 2013). From a modelling perspective, stronger positive cloud feedbacks over the southern ocean result in higher equilibrium climate sensitivities in Earth System Models (ESMs) from the recent 6th phase of the Coupled Model Intercomparison Project (CMIP6)
40 than in the earlier 5th phase (Zelinka et al., 2020; Wyser et al., 2020; Wang et al., 2021). Furthermore, ESMs usually lack the necessary spatial resolution and underlying physics to resolve the small floating ice shelves. For instance, coarse-resolution ESMs tend to project lower future melt changes compared to high-resolution regional projections (Kittel et al., 2021). This highlights the need for a more detailed quantification of the future cloud effects with high-resolution and polar-oriented models to evaluate uncertainties related to cloud properties on the projected Antarctic surface melt and resulting SLR contribution.

45 To understand how the SEB drives the differences in future summer surface melt over the Antarctic ice shelves, we force the regional climate model "Modèle Atmosphérique Régional" (MAR, Gallée and Schayes, 1994) with four ESMs from the CMIP5 (ACCESS1.3 and NorESM1-M) and CMIP6 (CNRM-CM6-1, CESM2) database using the highest greenhouse gas concentration pathways (respectively RCP8.5 and SSP585).

2 Methods

50 2.1 The regional atmospheric model MAR

The Modèle Atmosphérique Régional (MAR) is a hydrostatic regional climate model specifically developed for polar areas (Gallée and Schayes, 1994). MAR has often been used to study the present and future climates of both the Antarctic (Agosta



et al., 2019; Kittel et al., 2021) and Greenland ice sheets (Fettweis et al., 2020; Hofer et al., 2020). In this study, we used MARv3.11 whose specific adaptation and setup for the AIS is given in Agosta et al. (2019) and Kittel et al. (2021). The model
55 has been thoroughly evaluated over the AIS against near-surface observations from automatic weather stations (AWSs) (Datta et al., 2018; Mottram et al., 2021; Kittel et al., 2021; Amory et al., 2021) including radiative fluxes (Le Toumelin et al., 2021; Kittel, 2021), SMB measurements (Kittel et al., 2018; Agosta et al., 2019; Donat-Magnin et al., 2020; Mottram et al., 2021; Kittel et al., 2021), melt estimates derived from both satellites (Datta et al., 2018; Donat-Magnin et al., 2020) and AWSs (Kittel et al., 2021). MAR underestimates summer SWD by -6.9 W m^{-2} and LWD throughout the year by -9.9 W m^{-2} (Kittel, 2021).
60 While these biases seem significant compared to the future radiative forcing increase due to greenhouse gas concentration in 2100 ($+8.5 \text{ W m}^{-2}$ in RCP8.5 and SSP585, O'Neill et al., 2016), it is important to note that MAR correctly represents present Antarctic surface melt and near-surface temperatures (Kittel et al., 2021). This suggests a correct representation of the SEB through compensating turbulent fluxes and in general compensating errors whose impacts on the future SEB and melt is difficult to assess. Furthermore, this study aims to explain the projected spread in melt illustrated in previous studies using
65 MAR (Gilbert and Kittel, 2021; Kittel et al., 2021) rather than expanding on possible sources of misrepresentation of radiative fluxes in pre-existing simulations.

The cloud microphysics module of MAR solves conservation equations for five water species (cloud droplets, ice crystal, snow particles, rain drops, and specific humidity; Gallée, 1995) and the number of ice crystals (Messenger et al., 2004). The model takes into account the influence of these water species on cloud radiative properties (Gallée and Gorodetskaya, 2010) and
70 energy budget of each atmospheric layer in the radiative scheme inherited from the ECMWF ERA-40 reanalyses (Morcrette, 2002). MAR uses a broadband scheme for the longwave and shortwave radiations that integrates the values over the entire range of the two spectra. The radiative scheme uses the ice crystal, water vapour and cloud droplet concentrations from each atmospheric layer to determine the cloud optical properties. The snow particle concentration is implicitly taken into account by being partially included in the ice crystal concentration of each layer. The contribution of snow is expressed as an additional
75 concentration for ice crystal by assuming that the total ratio of snow and ice crystal is similar to the ratio of their effective radii, i.e. only 30% of snow is added in the ice crystal concentration input in the radiative scheme (Gallée and Gorodetskaya, 2010). The effect of rain droplets on radiation is neglected especially since the fall velocity of rain droplets used in MAR (Emde and Kahlig, 1989) induces that most of them reach the surface within one time-step of the radiative scheme. For shortwave radiation, the scheme uses the microphysics properties defined by Slingo (1989) for water clouds and by Fu (1996) for ice
80 clouds while water and ice cloud properties for longwave radiation are respectively based on parameterisations detailed in Lindner and Li (2000) and Fu et al. (1998).

2.1.1 Surface Energy Budget (SEB)

The surface module SISVAT (Soil Ice Snow Vegetation Atmosphere Transfer; De Ridder and Schayes, 1997; De Ridder, 1997; Gallée and Duynkerke, 1997; Gallée et al., 2001; Lefebvre et al., 2003) represents the evolution of snow and ice layer properties,
85 including their albedo based on CROCUS (Brun et al., 1992). SISVAT also deals with energy and mass exchanges between the atmosphere and the surface. SISVAT explicitly resolves the energy budget of 30 layers of snow and ice following (Gallée and



Duynkerke, 1997). In particular, the surface temperature evolution depends on the net shortwave (SWN), net longwave (LWN), sensible heat (SHF) and latent heat (LHF) fluxes, but also on snow melting, liquid water refreezing and thermal diffusion into layer(s) immediately below. The excess in energy is used to warm the snowpack or to melt the surface snow/ice if the surface temperature has reached 0°C. Liquid water resulting from melt or rain can percolate vertically and refreeze in the snowpack.

In this study, we have approximated the SEB (Eq. 1) as

$$: SEB = SWN + LWN + LHF + SHF. \quad (1)$$

with positive fluxes directed towards the surface.

We neglect snow thermal diffusion and liquid water refreezing energy as the focus of this study is on the atmospheric factors that contribute to melting. The snow thermal diffusion is also considered to be an order of magnitude smaller than other radiative and turbulent fluxes (Van As et al., 2005). Furthermore, the snow thermal diffusion does not contribute to surface melting as during melt conditions the surface layer at 0°C induces a downward heat flux toward colder underlying layers. The thin layers of snow at the surface cannot hold much liquid water, in contrast to the deeper and thicker layers of the snowpack into which liquid percolates. Refreezing therefore has a much higher warming potential in the deeper layers and only weakly contributes to surface melt. Finally, note that although refreezing increases with the production of liquid water via rain and surface melt, the projected increase in runoff indicates a decrease in the capacity of the snowpack to absorb liquid water (Kittel et al., 2021; Gilbert and Kittel, 2021) and thus the refreezing flux potential especially for larger warming rates. This highlights the predominant effect of the radiative - mostly SWN and LWN - or turbulent - mostly LHF and SHF fluxes and justifies the simplified SEB equation.

2.1.2 Forcing datasets and experiments

Large-scale conditions are prescribed every 6 hours at the MAR boundaries. The forcing fields include information about air temperature, specific humidity, zonal and meridional wind speeds, and at the surface, pressure, sea temperature, and sea ice concentration. MAR is also forced at the top of the atmosphere by large-scale temperature and wind components to constrain its atmospheric circulation (Agosta et al., 2019).

Most of the projections of the Antarctic melt have been performed in the frame of the 5th phase of the Coupled Intercomparison Project (CMIP5) (e.g., Trusel et al., 2015), while more recent climate models from CMIP6 now project stronger warmings at both local (Antarctic) and global scales. Both global climate models and Earth System Models are broadly referred to as ESMs hereafter without any distinction between several degrees of model sophistications. Although the plausibility of (very) high climate sensitivity in the CMIP6 ESMs remains low (Bjordal et al., 2020; Sherwood et al., 2020; Zhu et al., 2020), these ESMs enable the evaluation of the sensitivity of the AIS to high temperature increases. We selected models from both CMIP5 and CMIP6 using the highest emission scenario (i.e, RCP8.5 for CMIP5 models and SSP585 for CMIP6). These scenarios are equivalent in terms of radiative forcing (+8.5 W/m²) in 2100 (O’Neill et al., 2016). The detailed procedure that aims to select models that accurately represent the present Antarctic climate and maximise projected warming diversity can be found in Agosta et al. (2015), Barthel et al. (2020), and Kittel et al. (2021). In this study, MAR is forced by two CMIP5 models



120 (ACCESS1.3 and NorESM-1-M) and two CMIP6 models (CNRM-CM6-1 and CESM2). These ESMs represent a large range
of projected Antarctic warmings in 2100 qualified from weak (+3.2°C) to strong (+8.5°C) compared to the reference climate
of 1981–2010. We performed our projections with MAR using a 35km spatial resolution over 1975–2100, discarding the six
first years considered as spinup time. The evaluation of these MAR experiments can be found in Kittel et al. (2021).

The reference (present) period for computing the anomalies in this study is taken as the summer (December-January-
125 February, DJF) average from 1981 to 2010 for MAR over ice shelves (melt, SEB components, cloud amount and properties,
surface albedo) and ESMs over the Antarctic region, i.e 90°S–60°S (near-surface warming). Since more than 80% of the local
annual melt occurs in summer by 2100 (excepted over the Peninsula where it is more than 50%), we only discussed the summer
anomalies.

3 Results

130 3.1 Contributions to summer melt increase

Our four simulations project a summer melt increase over the ice shelves that strongly differs depending on the forcing ESM
during the 21st century (Fig. 1). We find a factor of ~ 3.9 between the lowest and highest cumulative melt anomalies over the
21st century, despite equivalent radiative forcing from greenhouse gases. MAR driven by NorESM1-M simulates a cumulated
melt increase of ~ 8000 Gt during the 21st century, while the increase reaches ~ 31400 Gt when MAR is driven by CNRM-
135 CM6-1. This spread in projected melt (despite an equivalent concentration pathway) is as large as differences in multimodel
estimates of Antarctic ice shelf surface melt between low- and high-concentration pathways by 2100 (Trusel et al., 2015; Kittel
et al., 2021).

The main increase in summer surface melt over ice shelves arises from LWN and SWN fluxes (Fig. 1). MAR projects a
strong increase in LWN as the surface receives more LWD by 2100 (Fig. S1). The mean cumulative LWN fluxes for the 21st
140 century correspond to 443.7 W m^{-2} in MAR driven by CNRM-CM6-1, i.e the higher melt projection. This represents $\sim 68\%$
of the projected net surface energy increase. In MAR driven by NorESM1-M (which produces the lowest melt increase), the
LWN increase is higher than the total net surface energy change. In the two other experiments (MAR driven by ACCESS1.3
and CESM2), LWN and SWN increase by approximately the same amount, contributing in a similar way to the projected
increase in total net surface energy.

145 Contrary to LWD, SWD fluxes decrease in all our simulations (Fig. S1). However, the albedo decreases as melt increases,
reducing shortwave reflection by the surface. This leads to positive potential melt contributions for SWN. MAR driven by
CNRM-CM6-1, CESM2, and to a lesser extent ACCESS1.3, suggest an equivalent SWN increase over the 21st century (~ 282
 W m^{-2} ; $\sim 269 \text{ W m}^{-2}$; and $\sim 205 \text{ W m}^{-2}$), whereas MAR driven by NorESM1-M projects only a $\sim 60 \text{ W m}^{-2}$ SWN contri-
bution to potential melt.

150 LWN contributions explain a large part of the melt anomaly differences between the simulations. Despite relatively similar
turbulent and shortwave cumulated anomalies with MAR driven by CESM2, the CNRM-CM6-1 experiment leads to larger
cumulative melt values that result from a larger LWN increase. Our CESM2 and CNRM-CM6-1 forced simulations reveal a

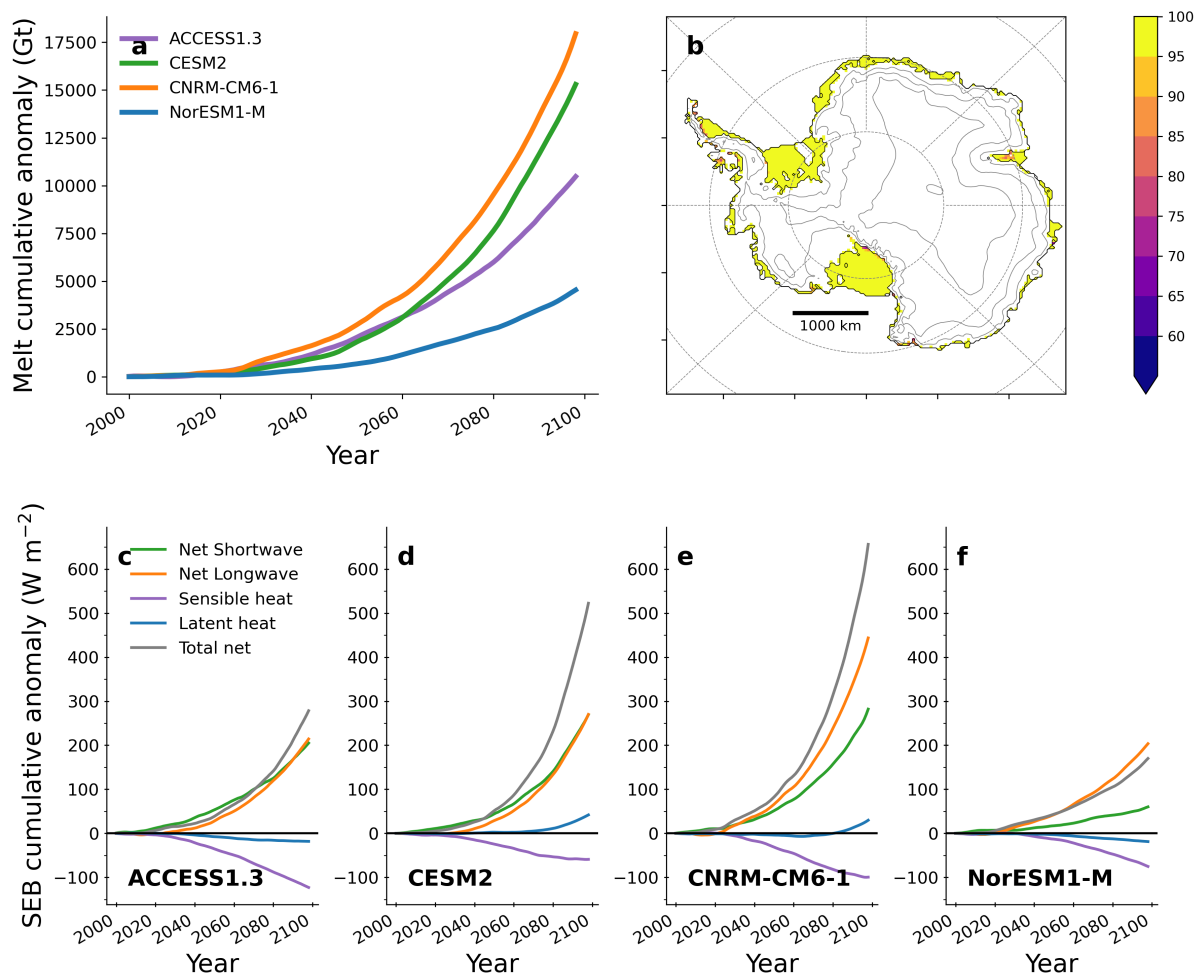


Figure 1. Cumulative summer melt (Gt) (a) and SEB components (c-f) (W m^{-2}) over the ice shelves projected by MAR forced by (c) ACCESS1.3, (d) CESM2, (e) CNRM-CM6-1, (f) NorESM1-M, compared to the reference 1981–2010 summer. The fixed ice mask over the ice shelves used by MAR in all the experiments is also represented (b).



factor of ~ 14 between the differences in SWN ($\sim 12 \text{ unitW m}^{-2}$) and LWN ($\sim 173 \text{ unitW m}^{-2}$) resulting in 2725 Gt more melting in MAR forced by CNRM-CM6-1. The same comparison between the ACCESS1.3 and CNRM-CM6-1 experiments
155 leads to similar conclusions, highlighting the large contribution of longwave differences for explaining differences in melt.

Turbulent fluxes play a minor role compared to the radiative fluxes (Fig. 1c,d,e,f). Although other studies (Kuipers Munneke et al., 2012, 2018; Lenaerts et al., 2017; Datta et al., 2019) have indicated that turbulent fluxes (especially SHF) can be the main drivers behind intense sporadic melt events occurring locally in peripheral regions of the ice sheet, our results indicate that their future change contribution is substantially lower than the radiation anomalies over ice shelves at the end the century.

160 Except for the NorESM1-M experiment where the melt increase remains weak, individual turbulent fluxes always have a lower contribution than radiative fluxes. While LHF does not notably change, SHF is projected to decrease, inducing a slightly negative contribution that we attribute to 1) a reduced thermal inversion between the atmosphere and the surface, and 2) weaker near-surface winds (See Section S2 in the supplementary materials). This is in agreement with Donat-Magnin et al. (2021) that projected a thickening of the future planetary boundary layer over ice shelves of West Antarctica, reducing temperature vertical
165 gradients and leading to a decrease in SHF.

The differences in projected melt and SEB in 2100 are partly linked with the warming sensitivity of each forcing ESM. As suggested by the global response of an ESM to increase in greenhouse gas concentration or equilibrium climate sensitivity (ECS, see supplement in Zelinka et al. (2020) for CMIP5 and CMIP6 models), MAR forced by NorESM1-M (ECS of 2.8) and ACCESS1.3 (ECS of 3.55) project a lower future melt than the two other experiments. Nonetheless, ECS does not wholly
170 explain the differences between the CESM2 (ECS of 5.15) and CNRM-CM6-1 (ECS of 4.9) experiments as the latter suggests a larger melt increase. This could be explained by the definition of ECS knowing that CNRM-CM6-1 projects a warming a little stronger over the Antarctic region ($+8.5^\circ\text{C}$ vs 7.7°C for CESM2 in 2100 compared to 1981-2010). However, MAR forced by this ESM still simulates a larger melt increase for the same warming rate than the other experiments (Fig. S4). This highlights that although model ECS contributes most strongly to uncertainty in melt and SEB, other local physical mechanisms have to
175 be involved in addition to ESM warming rates. We will therefore analyse the factors behind the LWD differences, focusing especially on the CNRM-CM6-1 and CESM2 experiments having in mind their (relatively-) close ECS and regional Antarctic warmings.

3.2 Factors behind the differences in LWD

The projected LWD increases in each experiment are mainly due to higher atmospheric temperature, larger greenhouse gas
180 concentrations including water vapour, and optically thicker clouds. We perform our MAR projections using RCP8.5 for CMIP5 forcings and SSP585 for CMIP6 forcings. Despite differences in specific anthropogenic greenhouse gas concentrations, these two scenarios result in the same radiative forcing in 2100 ($+8.5 \text{ W m}^{-2}$) suggesting a low influence on LWD. We will therefore analyse the contribution of the remaining factors - atmospheric temperature, water vapour and cloud properties.



3.2.1 Changes in atmospheric temperature and water vapour

185 For a similar warming rate, the differences in projected atmospheric temperatures and water vapour only contribute to small
differences in LWD. The increase in temperature of the atmosphere related to the sensitivity of the ESM forcing, determines the
absolute increases and differences (Fig. S5 and Table S1). This is notably highlighted by the differences between MAR forced
by NorESM1-M and the other experiments. However, temperature alone is not sufficient to explain the large LWD differences
for the same warming rate (Fig. S5). Higher atmospheric water vapour content favour higher LWD but all MAR experiments
190 project similar increases in water vapour for the same warming rate following the Clausius-Clapeyron relation (Fig. S6).

The absolute increases and differences in LWD are linked with the temperature of the atmosphere. The climatic sensitivity of
each ESM (as indicated by their ECS) influences the atmospheric air temperature and water vapour concentration for a given
future time period, explaining melt changes that are projected to be weak for the lower (NorESM1-M), intermediate (AC-
CESS1.3) or large (CNRM-CM6-1 and CESM2) melt experiments by 2100. Accordingly, the predominant factor contributing
195 to melt differences is the warming projected by each ESM, highlighting the importance of multi-model projections for a better
assessment of uncertainties. However, comparing our results for the same rate of warming (see CNRM-CM6-1 and CESM2
ECS or local projected warming above) suggests the importance of other physical processes, such as the role of clouds, for
explaining the large potential melt differences projected for the same rate of warming.

3.2.2 Changes in cloud properties

200 The cloud contribution to LWD mainly depends on their own longwave emissivity. The latter can be modified by the COD
and therefore cloud phase. Furthermore, a larger cloud cover also favours larger LWD values even for unchanged physical
properties (ie, COD). The MAR experiments project a larger cloud cover and also more opaque clouds that both enhance LWD
(Fig. 2) and decrease SWD (Fig. S1).

The mean summer cloud cover (CC) and COD increase during the 21st century (Fig 2). While MAR driven by ACCESS1.3,
205 NorESM1-M, and CESM2 have similar CC increases (between $\sim 2.5\%$ and $\sim 3\%$), the CNRM-CM6-1 experiment (ie., with
the strongest melt) reveals the largest cloud cover increase with 7% more frequent clouds during the southern summer. This
is a factor of two compared to the other projections. In the same way, COD increases starting from ~ 2020 with a factor ~ 5
between the smallest (NorESM1-M) and the largest (CNRM-CM6-1) increases. The mean summer COD presented here is a
diagnostic, post-processed variable computed by taking into account ice and liquid particles only (snow particles are neglected).
210 It is computed with all the values including indiscriminately both clear and cloudy sky conditions. While any increase in CC
will also be translated into a COD increase, Figure 2 shows that COD and CC anomalies do not co-vary in the same way
between models. This suggests that non-similar changes in cloud phase properties also contribute to LWD and melt differences
for the same warming rate. Note that the COD discussed here is not the exact same value as computed in the radiative scheme
(not available in our simulations) and therefore we only use it here as an indicative variable to represent cloud phase properties
215 that can be easily compared to CC.

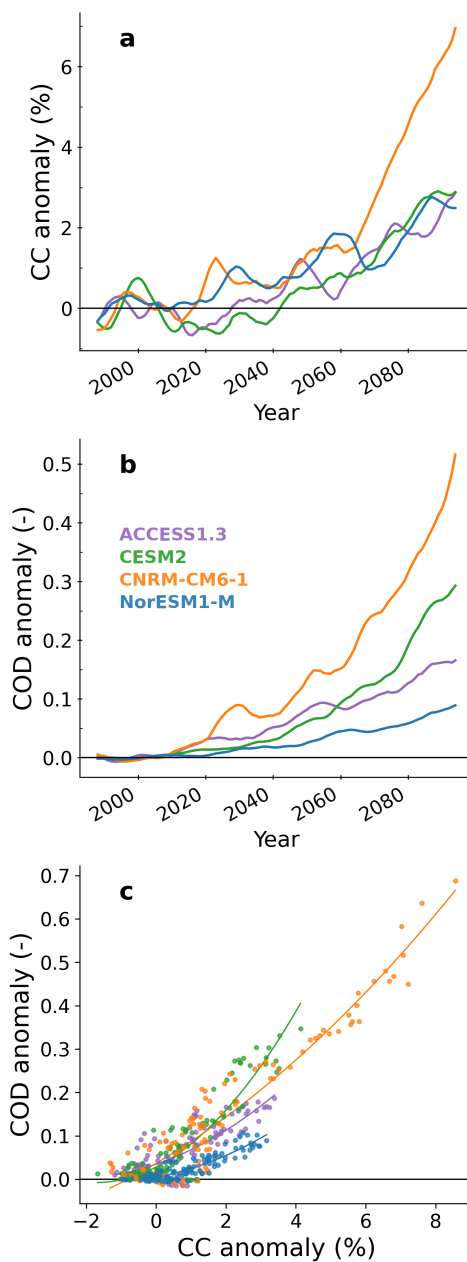


Figure 2. Changes in mean summer cloud cover (%) (a), mean summer cloud optical depth (-) (b), Changes in mean summer cloud optical depth (-) compared with changes mean summer cloud cover (%) (c) projected by MAR forced by ACCESS1.3 (purple), CESM2 (green), CNRM-CM6-1 (orange), and NorESM1-M (blue) compared to the present summer climate (1981–2010).



Although COD is projected to increase in all our simulations, MAR driven by CNRM-CM6-1 suggests a stronger increase (up to ~ 0.7) around 2040–2060, which corresponds to clouds twice as opaque than clouds simulated in the MAR-CESM2 experiment (i.e., the simulation with the second-largest COD increase). We find a strong association between LWD and COD changes for each experiment ($R^2 > 0.98$; $p < 0.01$, Fig. 3). However, the function between longwave cloud emissivity and COD shows a saturation of LWD for large COD increases. This however does not suggest a fully opaque atmosphere to longwave radiation due to clouds, as the emissivity could still increase until cloud cover reaches 100%.

We extrapolate our projections based on equations from Fig. 3, to find that increase in LWD associated to an increase in COD would stop when COD equals 1.22 (+0.96 compared to present values) (ACCESS1.3), 1.10 (+0.96) (NorESM1-M), 1.78 (+0.91) (CNRM-CM6-1), 1.2 (+0.89) (CESM2). Since these values are not reached before 2100 in our simulations, the future LWD increase is supposed to remain sensitive to cloud optical properties during the whole 21st century, including for high warming rates as projected by CNRM-CM6-1 and CESM2. While higher temperatures lead to larger COD increases, Figure S7 demonstrates that the future changes are not only a direct consequence of the atmospheric warming. For instance, MAR driven by CNRM-CM6-1 simulates stronger changes in COD than other experiments for equivalent near-surface warming rates over the ice shelves. This again highlights the predominant influence of the ESM warming as the main driver of melt differences but also the amplifying role of clouds.

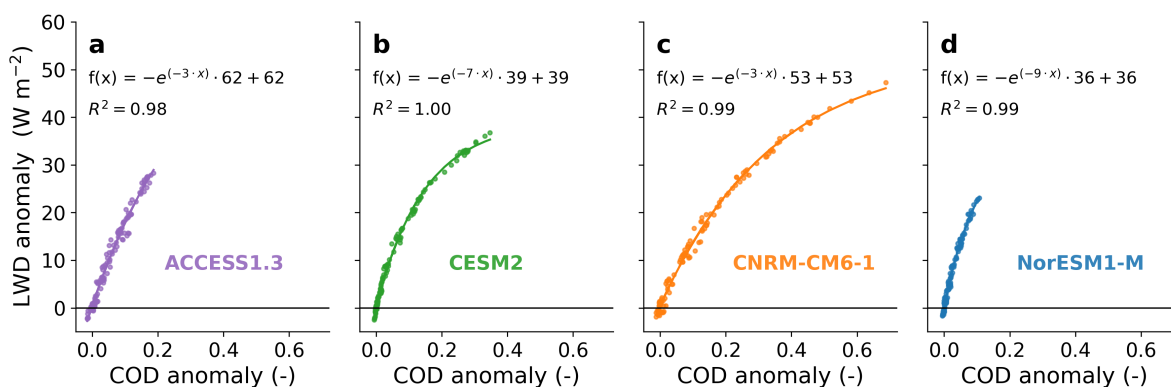


Figure 3. Relation between LWD summer anomalies and COD summer anomalies. Summer longwave downwelling radiation (W m^{-2}) versus mean cloud optical depth anomalies during summer (-) projected by MAR driven by ACCESS1.3 (a), CESM2 (b), CNRM-CM6-1 (c), and NorESM1-M (d) compared to the summer reference period (1981–2010). The exponential regression as well as corresponding determination coefficient (R^2 , $p < 0.01$) is indicated for each experiment. A 5-year running mean has been applied on the anomalies.

3.2.3 Changes in cloud particle water phase and mass

MAR projects an increase in cloud particle contents and changes in phase distributions over the ice shelves that differ between the simulations, resulting in different cloud optical properties (Fig. 4a,c). Over 2071–2100, the summer mean solid water path (SWP, the mean total amount of ice and snow content in the atmosphere averaged for every summer) increases similarly



235 among experiments with anomalies between 18.2 g m^{-2} and 35.4 g m^{-2} which represents a factor of 2.1 between the lowest (NorESM1-M) and the highest increase (CESM2). This increase in the CESM2 experiment represents an increase of +33% compared to present values and does not result from an underestimation over the present climate, as all the experiments starts with similar SWP values around 100 g m^{-2} . While all projections simulate a higher liquid water path (LWP, equivalent of SWP for water droplet content) in the future, large differences persist in the anomalies. MAR driven by CNRM-CM6-1 projects a
240 stronger increase in LWP (11.1 g m^{-2}) that is 8.5 larger than the increase in the NorESM1-M experiment (1.3 g m^{-2}) over 2071–2100.

The different increases in LWP control the spread in projected LWD for a same warming rate. This results from the strong dependence of cloud emissivity to their liquid water content (Stephens, 1984; Bennartz et al., 2013). While the CESM2 experiment suggests slightly larger changes in SWP than the CNRM-CM6-1 experiment, the latter projects more liquid-
245 containing clouds (higher LWP) resulting in more opaque clouds (higher COD and then higher LWD) for the same warming rate (Fig. 4b,d). This analysis highlights the strong influence of cloud water phase for explaining melt differences projected for the same warming rate over Antarctic ice shelves.

The projected cloud phase differences are explained by the preferential increase of either water and rain droplets or ice and snow particles at a same warming rate. Over 2071–2100, both the vertically-averaged atmospheric changes in humidity and
250 temperature projected by MAR driven by CESM2 and CNRM-CM6-1 are similar over the ice shelves (Tab. S2). This enables a direct comparison removing the influence of global warming on potential differences. However, they differ in their vertical structure (Fig. 5). At the lateral boundaries, the CESM2 experiment reveals a future stronger increase in specific humidity above 2000 masl than the CNRM-CM6-1 one. The pattern is opposite below 2000 masl where the future CNRM-CM6-1 atmosphere is characterised by stronger low-level humidity advection (Fig. 5a). High- and mid-level humidity advection
255 favours the formation of snow particles (Fig. 5b), while low-level humidity advection, where the temperature is higher, leads to the formation of more water droplets (Fig. 5c). The formation of either snow (and ice) particles (CESM2) or water droplets (CNRM-CM6-1) when saturation is reached results in differences in SWP and LWP that further induces changes in LWD. The preferential future increase in low-level water droplets in the CNRM-CM6-1 experiment finally induces a stronger surface melt over the ice shelves than the CESM2 experiment despite a similar regional warming rate. The preferential increase in either
260 cloud water droplets or snow particles also explains why MAR driven by CNRM-CM6-1 simulates more liquid precipitation than when driven by CESM2 and conversely for solid precipitation (see the Fig. 7 in Kittel et al. (2021)).

3.3 Enhanced SWD absorption due to clouds

The surface is projected to absorb more shortwave despite decreased SWD (Fig. S1). The excess energy at the surface due to LWD warms and melts snow. This in turn promotes snow grain metamorphism that combined with refreezing of liquid
265 meltwater, lowers the albedo and ultimately favours SWD absorption. This effect dominates over the decrease in SWD caused by the more numerous and also more opaque clouds. We only find a small albedo decrease in the NorESM1-M experiment (Fig. 6) suggesting a low melt-albedo feedback explained by the weak projected increase in melt. On the contrary, the albedo is projected to strongly decrease when MAR is forced by CNRM-CM6-1 leading to large anomalies in SWN. In this experiment,

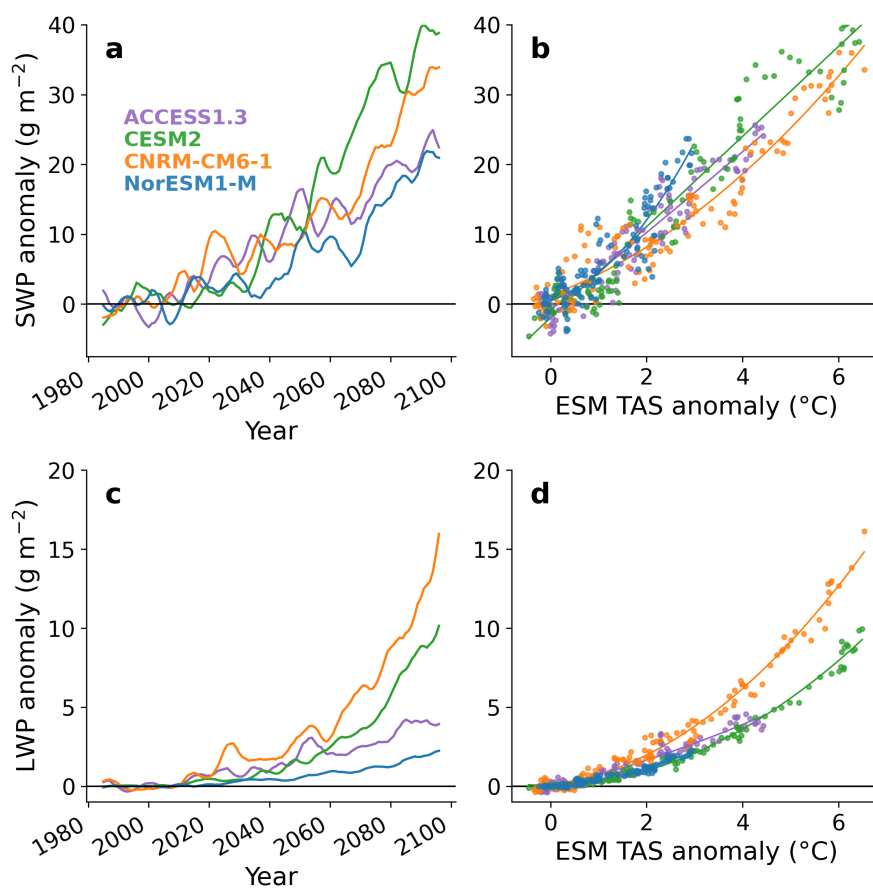


Figure 4. Anomalies compared to the present summer climate (1981–2010) projected by MAR forced by ACCESS1.3 (purple), CESM2 (green), CNRM-CM6-1 (orange), and NorESM1-M (blue) of mean summer solid (ice and snow) water path (g m^{-2}) (a), mean summer liquid water path (g m^{-2}) (c). Mean summer solid (ice and snow) water path (g m^{-2}) (b) and , mean summer liquid water path (g m^{-2}) (d) projected by MAR compared to summer near-surface temperature anomaly from the forcing ESMs between 90°S - 60°S ($^{\circ}\text{C}$).

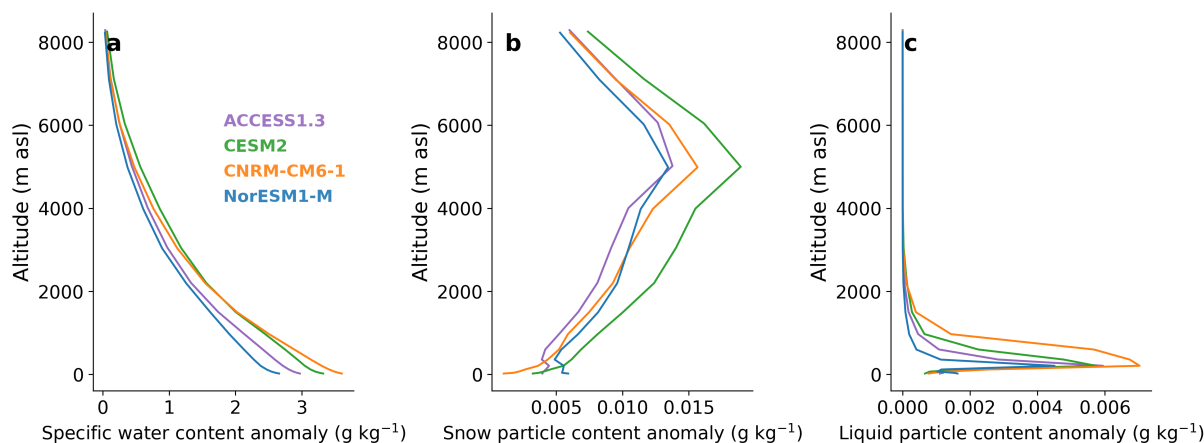


Figure 5. Changes in mean summer vertical specific humidity profiles over the boundaries (a), snow particle content (b), and water droplet particle content (c) (g kg^{-1}) over the ice shelf in 2071–2100 compared to 1981–2010 projected by ACCESS1.3 (purple), CESM2 (green), CNRM-CM6-1 (orange), and NorESM1-M (blue).

the mean summer 2-m temperature over the ice shelves nearly reaches 0°C at the end of the 21st century (-0.9°C over 270 2095–2100). Similarly, the albedo is projected to notably decrease in the CESM2 experiment. However, the same warming rate results in a smaller albedo decrease in this experiment than in CNRM-CM6-1. As melt differences between these two simulations mainly arise from LWD and more liquid-containing clouds, this further highlights the importance of the cloud radiative effect on melt and albedo feedbacks.

The influence of clouds on absorbed SWD mainly depends on the surface albedo but also on the rate at which SWD is 275 projected to decrease due to an increase in CC and/or COD (Bintanja and van den Broeke, 1996). In warmer climates after 2100, clouds could be more reflective than the ice-covered surface, as summer surface albedo is projected to decrease. These warmer conditions could reverse the summer cloud radiative effect, reducing melt, similarly as over the dark ablation zone of the Greenland Ice Sheet (Hofer et al., 2017; Wang et al., 2019), suggesting a growing importance of surface albedo in determining the future cloud radiative effect.

280 4 Conclusions

We investigate in this study the physical drivers of summer melt differences over the Antarctic ice shelves by 2100 between four dynamical downscaling of CMIP5 and CMIP6 ESMs with MAR under the highest greenhouse gas concentration pathways (RCP8.5 and SSP585). Our results highlight the important role of clouds in amending future Antarctic ice shelf melt. The main differences in melt between simulations arise from LWN and SWN fluxes while non-radiative fluxes play only a minor 285 role. Among the radiative fluxes, LWN contributes the most to the differences in melt between our different experiments. Furthermore, we highlight the importance of total cloud water content and phase to explain the differences in projected melt for

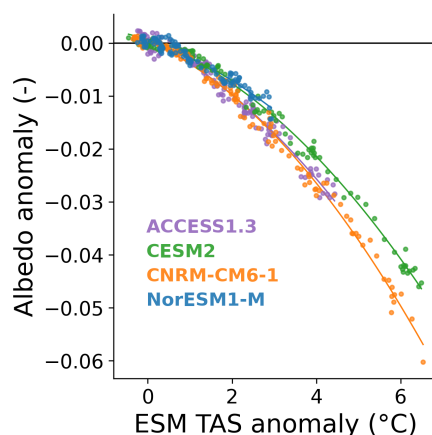


Figure 6. Association between mean summer albedo anomalies (-) projected by MAR over the Antarctic ice shelves and summer near-surface air temperature anomalies projected by the respective ESM forcing (ACCESS1.3 (purple), CESM2 (green), CNRM-CM6-1 (orange), and NorESM1-M (blue)) between 90°S–60°S. The reference period is 1981–2010.

a given warming. More liquid-water-containing clouds induce a stronger increase in LWD that enhances meltwater production but also favours SWD absorption due to the melt-albedo feedback, further increasing melt. Finally, we find that this preferential increase in water droplets results from a stronger increase in low-level humidity advection rather than high- and mid-level advection that tends to favour the formation of snow and ice particles.

While it is common to assess the Antarctic contribution to SLR associated with specific warming rates (e.g., Pattyn et al., 2018), liquid-containing clouds could lead to large uncertainties even for the same warming rate. For instance, the larger melt rate projected in the CNRM-CM6-1 experiment could lead to 32% (relative augmentation, or 19% in absolute values) of areas susceptible to hydrofracturing collapses than the CESM2 experiment (Gilbert and Kittel, 2021) despite a similar global warming. In 2100, MAR driven by CNRM-CM6-1 projects that around 99% (76% over 2071–2100) of the Antarctic ice shelves could be vulnerable to surface melt-driven disintegration. Without the buttressing effect of these ice shelves, Antarctic glaciers accelerate, increasing their discharge into the ocean and raising global sea level (Sun et al., 2016). This suggests that clouds are projected to have a strong effect on determining the Antarctic contribution to SLR.

While MAR projections reveal significant melt differences using different ESM forcings (Kittel et al., 2021; Gilbert and Kittel, 2021), we emphasize here that none of these projections is more plausible than any other and that the purpose of this study is, on the contrary, to highlight the physical factors that can lead to large uncertainties in Antarctic melt projections. The warming projected by the ESM forcing is the main factor controlling absolute melt differences, but we suggest that clouds and their phase are important factors contributing to the spread in melt and by extension surface mass balance projections of the AIS for the same warming rate. Furthermore, a recent study with MAR (Le Toumelin et al., 2021) has revealed significant changes in LWD due to drifting snow, a process not modelled in our study, suggesting that drifting snow could further contribute to the spread in melt projections. While climate models (including MAR) tend to poorly simulate clouds over the present (Gallée



and Gorodetskaya, 2010; King et al., 2015; Silber et al., 2019; Gilbert et al., 2020; Mattingly et al., 2020; Mülmenstädt et al., 2021), our study stresses the need to improve cloud representation in climate models to better constrain SLR projections.

Code and data availability. The MAR code used in this study is tagged as v3.11.1 on <https://gitlab.com/Mar-Group/MAR>. Instructions to
310 download the MAR code are provided on <https://www.mar.cnrs.fr>. The MAR version used for the present work is tagged as v3.11.1. The
MAR outputs used in this study will be stored on Zenodo after the eventual acceptance of the paper and are available on:

<ftp://ftp.climato.be/limato/ckittel/MARv3.11/SEB/>

Other higher-frequency MAR results and Python scripts are also available upon request by email (ckittel@uliege.be).

Author contributions. CK designed the study, ran the simulations, made the plots, performed the analysis and wrote the manuscript. CAM,
315 XF provided important guidance while all the authors (CK, ChA, SH, CÉA, NCJ, EG, LLT, HG and XF) discussed and revised the manuscript.

Competing interests. The authors declare that they have no conflict of interest.

Acknowledgements. We acknowledge the World Climate Research Programme's Working Group on Coupled Modelling, which is responsible for CMIP, and we thank the climate modelling groups for producing their model output and making it available.

320 Computational resources have been provided by the Consortium des Équipements de Calcul Intensif (CÉCI), funded by the Fonds de la
Recherche Scientifique de Belgique (F.R.S. – FNRS) under grant no. 2.5020.11 and the Tier-1 supercomputer (Zenobe) of the Fédération
Wallonie Bruxelles infrastructure funded by the Walloon Region under grant agreement no. 1117545. This research has been supported by
F.R.S.-FNRS, the Fonds Wetenschappelijk Onderzoek-Vlaanderen (FWO) under the EOS project no. O0100718F.



References

- Agosta, C., Fettweis, X., and Datta, R.: Evaluation of the CMIP5 models in the aim of regional modelling of the Antarctic surface mass balance, *The Cryosphere*, 9, 2311–2321, 2015.
- Agosta, C., Amory, C., Kittel, C., Orsi, A., Favier, V., Gallée, H., van den Broeke, M. R., Lenaerts, J., van Wessem, J. M., van de Berg, W. J., et al.: Estimation of the Antarctic surface mass balance using the regional climate model MAR (1979–2015) and identification of dominant processes, *The Cryosphere*, 13, 281–296, 2019.
- Amory, C., Kittel, C., Le Toumelin, L., Agosta, C., Delhasse, A., Favier, V., and Fettweis, X.: Performance of MAR (v3.11) in simulating the drifting-snow climate and surface mass balance of Adélie Land, East Antarctica, *Geoscientific Model Development*, 14, 3487–3510, <https://doi.org/10.5194/gmd-14-3487-2021>, <https://gmd.copernicus.org/articles/14/3487/2021/>, 2021.
- Barrett, A. I., Hogan, R. J., and Forbes, R. M.: Why are mixed-phase altocumulus clouds poorly predicted by large-scale models? Part 1. Physical processes, *Journal of Geophysical Research: Atmospheres*, 122, 9903–9926, 2017.
- Barthel, A., Agosta, C., Little, C. M., Hattermann, T., Jourdain, N. N., Goelzer, H., Nowicki, S., Seroussi, H., Straneo, F., and Bracegirdle, T. T.: CMIP5 model selection for ISMIP6 ice sheet model forcing: Greenland and Antarctica, *The Cryosphere*, 14, 855–879, 2020.
- Bennartz, R., Shupe, M., Turner, D., Walden, V., Steffen, K., Cox, C., Kulie, M., Miller, N., and Pettersen, C.: July 2012 Greenland melt extent enhanced by low-level liquid clouds, *Nature*, 496, 83–86, 2013.
- Bintanja, R. and van den Broeke, M. R.: The influence of clouds on the radiation budget of ice and snow surfaces in Antarctica and Greenland in summer, *International Journal of Climatology: A Journal of the Royal Meteorological Society*, 16, 1281–1296, 1996.
- Bjorndal, J., Storelvmo, T., Alterskjær, K., and Carlsen, T.: Equilibrium climate sensitivity above 5 C plausible due to state-dependent cloud feedback, *Nature Geoscience*, 13, 718–721, 2020.
- Boucher, O., Randall, D., Artaxo, P., Bretherton, C., Feingold, G., Forster, P., Kerminen, V.-M., Kondo, Y., Liao, H., Lohmann, U., et al.: Clouds and aerosols, in: *Climate change 2013: the physical science basis. Contribution of Working Group I to the Fifth Assessment Report of the Intergovernmental Panel on Climate Change*, pp. 571–657, Cambridge University Press, 2013.
- Bromwich, D. H., Nicolas, J. P., Hines, K. M., Kay, J. E., Key, E. L., Lazzara, M. A., Lubin, D., McFarquhar, G. M., Gorodetskaya, I. V., Grosvenor, D. P., et al.: Tropospheric clouds in Antarctica, *Reviews of Geophysics*, 50, 2012.
- Brun, E., David, P., Sudul, M., and Brunot, G.: A numerical model to simulate snow-cover stratigraphy for operational avalanche forecasting, *Journal of Glaciology*, 38, 13–22, 1992.
- Datta, R. T., Tedesco, M., Agosta, C., Fettweis, X., Kuipers Munneke, P., and Broeke, M. R.: Melting over the northeast Antarctic Peninsula (1999–2009): evaluation of a high-resolution regional climate model, *The Cryosphere*, 12, 2901–2922, 2018.
- Datta, R. T., Tedesco, M., Fettweis, X., Agosta, C., Lhermitte, S., Lenaerts, J. T., and Wever, N.: The effect of Foehn-induced surface melt on firn evolution over the northeast Antarctic peninsula, *Geophysical Research Letters*, 46, 3822–3831, 2019.
- De Ridder, K.: Radiative transfer in the IAGL land surface model, *Journal of Applied Meteorology*, 36, 12–21, 1997.
- De Ridder, K. and Schayes, G.: The IAGL land surface model, *Journal of applied meteorology*, 36, 167–182, 1997.
- Donat-Magnin, M., Jourdain, N. C., Gallée, H., Amory, C., Kittel, C., Fettweis, X., Wille, J. D., Favier, V., Drira, A., and Agosta, C.: Interannual variability of summer surface mass balance and surface melting in the Amundsen sector, West Antarctica, *The Cryosphere*, 14, 229–249, 2020.



- Donat-Magnin, M., Jourdain, N. C., Kittel, C., Agosta, C., Amory, C., Gallée, H., Krinner, G., and Chekki, M.: Future surface mass balance and surface melt in the Amundsen sector of the West Antarctic Ice Sheet, *The Cryosphere*, 15, 571–593, <https://doi.org/10.5194/tc-15-571-2021>, <https://tc.copernicus.org/articles/15/571/2021/>, 2021.
- Emde, K. D. and Kahlig, P.: Comparison of the observed 19th July 1981, Montana thunderstorm with results of a one-dimensional cloud model using Kessler parameterized microphysics, in: *Annales geophysicae. Atmospheres, hydrospheres and space sciences*, vol. 7(4), pp. 405–414, 1989.
- Fettweis, X., Hofer, S., Krebs-Kanzow, U., Amory, C., Aoki, T., Berends, C. J., Born, A., Box, J. E., Delhasse, A., Fujita, K., Gierz, P., Goelzer, H., Hanna, E., Hashimoto, A., Huybrechts, P., Kapsch, M.-L., King, M. D., Kittel, C., Lang, C., Langen, P. L., Lenaerts, J. T. M., Liston, G. E., Lohmann, G., Mernild, S. H., Mikolajewicz, U., Modali, K., Mottram, R. H., Niwano, M., Noël, B., Ryan, J. C., Smith, A., Streffing, J., Tedesco, M., van de Berg, W. J., van den Broeke, M., van de Wal, R. S. W., van Kampenhout, L., Wilton, D., Wouters, B., Ziemen, F., and Zolles, T.: GrSMBMIP: intercomparison of the modelled 1980–2012 surface mass balance over the Greenland Ice Sheet, *The Cryosphere*, 14, 3935–3958, 2020.
- Fu, Q.: An accurate parameterization of the solar radiative properties of cirrus clouds for climate models, *Journal of Climate*, 9, 2058–2082, 1996.
- Fu, Q., Yang, P., and Sun, W.: An accurate parameterization of the infrared radiative properties of cirrus clouds for climate models, *Journal of climate*, 11, 2223–2237, 1998.
- Gallée, H.: Simulation of the mesocyclonic activity in the Ross Sea, Antarctica, *Monthly Weather Review*, 123, 2051–2069, 1995.
- Gallée, H. and Duynkerke, P. G.: Air-snow interactions and the surface energy and mass balance over the melting zone of west Greenland during the Greenland Ice Margin Experiment, *Journal of Geophysical Research: Atmospheres*, 102, 13 813–13 824, 1997.
- Gallée, H. and Gorodetskaya, I. V.: Validation of a limited area model over Dome C, Antarctic Plateau, during winter, *Climate dynamics*, 34, 61, 2010.
- Gallée, H. and Schayes, G.: Development of a three-dimensional meso- γ primitive equation model: katabatic winds simulation in the area of Terra Nova Bay, Antarctica, *Monthly Weather Review*, 122, 671–685, 1994.
- Gallée, H., Guyomarc’h, G., and Brun, E.: Impact of snow drift on the antarctic ice sheet surface mass balance: Possible sensitivity to snow-surface properties, *Boundary-Layer Meteorology*, 99, 1–19, 2001.
- Ghiz, M. L., Scott, R. C., Vogelmann, A. M., Lenaerts, J. T. M., Lazzara, M., and Lubin, D.: Energetics of surface melt in West Antarctica, *The Cryosphere*, 15, 3459–3494, 2021.
- Gilbert, E. and Kittel, C.: Surface Melt and Runoff on Antarctic Ice Shelves at 1.5° C, 2° C, and 4° C of Future Warming, *Geophysical Research Letters*, 48, e2020GL091 733, 2021.
- Gilbert, E., Orr, A., King, J. C., Renfrew, I., Lachlan-Cope, T., Field, P., and Boutle, I.: Summertime cloud phase strongly influences surface melting on the Larsen C ice shelf, Antarctica, *Quarterly Journal of the Royal Meteorological Society*, 146, 1575–1589, 2020.
- Gorodetskaya, I., Kneifel, S., Maahn, M., Van Tricht, K., Thiery, W., Schween, J., Mangold, A., Crewell, S., and Van Lipzig, N.: Cloud and precipitation properties from ground-based remote-sensing instruments in East Antarctica, *Cryosphere*, 9, 285–304, 2015.
- Hines, K. M., Bromwich, D. H., Wang, S.-H., Silber, I., Verlinde, J., and Lubin, D.: Microphysics of summer clouds in central West Antarctica simulated by the Polar Weather Research and Forecasting Model (WRF) and the Antarctic Mesoscale Prediction System (AMPS)., *Atmospheric Chemistry & Physics*, 19, 2019.
- Hofer, S., Tedstone, A. J., Fettweis, X., and Bamber, J. L.: Decreasing cloud cover drives the recent mass loss on the Greenland Ice Sheet, *Science Advances*, 3, e1700 584, 2017.



- Hofer, S., Tedstone, A. J., Fettweis, X., and Bamber, J. L.: Cloud microphysics and circulation anomalies control differences in future Greenland melt, *Nature Climate Change*, 9, 523–528, 2019.
- Hofer, S., Lang, C., Amory, C., Kittel, C., Delhasse, A., Tedstone, A., and Fettweis, X.: Greater Greenland Ice Sheet contribution to global sea level rise in CMIP6, *Nature communications*, 11, 1–11, 2020.
- 400 King, J., Gadian, A., Kirchgassner, A., Kuipers Munneke, P., Lachlan-Cope, T., Orr, A., Reijmer, C., van den Broeke, M., Van Wessem, J., and Weeks, M.: Validation of the summertime surface energy budget of Larsen C Ice Shelf (Antarctica) as represented in three high-resolution atmospheric models, *Journal of Geophysical Research: Atmospheres*, 120, 1335–1347, 2015.
- Kittel, C.: Present and future sensitivity of the Antarctic surface mass balance to oceanic and atmospheric forcings: insights with the regional climate model MAR, Ph.D. thesis, University of Liège, Liège, <http://hdl.handle.net/2268/258491>, 2021.
- 405 Kittel, C., Amory, C., Agosta, C., Delhasse, A., Doutreloup, S., Huot, P.-V., Wyard, C., Fichet, T., and Fettweis, X.: Sensitivity of the current Antarctic surface mass balance to sea surface conditions using MAR, *The Cryosphere*, 12, 3827–3839, 2018.
- Kittel, C., Amory, C., Agosta, C., Jourdain, N. C., Hofer, S., Delhasse, A., Doutreloup, S., Huot, P.-V., Lang, C., Fichet, T., and Fettweis, X.: Diverging future surface mass balance between the Antarctic ice shelves and grounded ice sheet, *The Cryosphere*, 15, 1215–1236, <https://doi.org/10.5194/tc-15-1215-2021>, 2021.
- 410 Kuipers Munneke, P., Van den Broeke, M., King, J., Gray, T., and Reijmer, C.: Near-surface climate and surface energy budget of Larsen C ice shelf, *Antarctic Peninsula*, *The Cryosphere*, 6, 353–363, 2012.
- Kuipers Munneke, P., Luckman, A., Bevan, S., Smeets, C., Gilbert, E., Van den Broeke, M., Wang, W., Zender, C., Hubbard, B., Ashmore, D., et al.: Intense winter surface melt on an Antarctic ice shelf, *Geophysical Research Letters*, 45, 7615–7623, 2018.
- Lachlan-Cope, T.: Antarctic clouds, *Polar Research*, 29, 150–158, 2010.
- 415 Le Toumelin, L., Amory, C., Favier, V., Kittel, C., Hofer, S., Fettweis, X., Gallée, H., and Kayetha, V.: Sensitivity of the surface energy budget to drifting snow as simulated by MAR in coastal Adelie Land, Antarctica, *The Cryosphere*, 15, 3595–3614, 2021.
- Lefebvre, F., Gallée, H., van Ypersele, J.-P., and Greuell, W.: Modeling of snow and ice melt at ETH Camp (West Greenland): A study of surface albedo, *Journal of Geophysical Research: Atmospheres*, 108, 2003.
- Lenaerts, J., Lhermitte, S., Drews, R., Ligtenberg, S., Berger, S., Helm, V., Smeets, C., Van Den Broeke, M., Van De Berg, W. J., Van Meijgaard, E., et al.: Meltwater produced by wind–albedo interaction stored in an East Antarctic ice shelf, *Nature climate change*, 7, 58–62, 2017.
- Lhermitte, S., Sun, S., Shuman, C., Wouters, B., Pattyn, F., Wuite, J., Berthier, E., and Nagler, T.: Damage accelerates ice shelf instability and mass loss in Amundsen Sea Embayment, *Proceedings of the National Academy of Sciences*, <https://doi.org/10.1073/pnas.1912890117>, <https://www.pnas.org/content/early/2020/09/08/1912890117>, 2020.
- 425 Lindner, T. and Li, J.: Parameterization of the optical properties for water clouds in the infrared, *Journal of Climate*, 13, 1797–1805, 2000.
- Mattingly, K. S., Mote, T. L., Fettweis, X., Van As, D., Van Tricht, K., Lhermitte, S., Pettersen, C., and Fausto, R. S.: Strong summer atmospheric rivers trigger Greenland Ice Sheet melt through spatially varying surface energy balance and cloud regimes, *Journal of Climate*, 33, 6809–6832, 2020.
- 430 Messenger, C., Gallée, H., and Brasseur, O.: Precipitation sensitivity to regional SST in a regional climate simulation during the West African monsoon for two dry years, *Climate Dynamics*, 22, 249–266, 2004.
- Morcrette, J.-J.: The Surface Downward Longwave Radiation in the ECMWF Forecast System, *Journal of Climate*, 15, 1875–1892, 2002.



- Mottram, R., Hansen, N., Kittel, C., van Wessem, J. M., Agosta, C., Amory, C., Boberg, F., van de Berg, W. J., Fettweis, X., Gossart, A., van Lipzig, N. P. M., van Meijgaard, E., Orr, A., Phillips, T., Webster, S., Simonsen, S. B., and Souverijns, N.: What is the surface mass balance of Antarctica? An intercomparison of regional climate model estimates, *The Cryosphere*, 15, 3751–3784, 2021.
- 435 Mülmenstädt, J., Salzmann, M., Kay, J. E., Zelinka, M. D., Ma, P.-L., Nam, C., Kretschmar, J., Hörnig, S., and Quaas, J.: An underestimated negative cloud feedback from cloud lifetime changes, *Nature Climate Change*, 11, 508–513, 2021.
- Nicolas, J. P., Vogelmann, A. M., Scott, R. C., Wilson, A. B., Cadetdu, M. P., Bromwich, D. H., Verlinde, J., Lubin, D., Russell, L. M., Jenkinson, C., et al.: January 2016 extensive summer melt in West Antarctica favoured by strong El Niño, *Nature Communications*, 8, 15 799, 2017.
- 440 O’Neill, B. C., Tebaldi, C., van Vuuren, D., Eyring, V., Friedlingstein, P., Hurtt, G., Knutti, R., Kriegler, E., Lamarque, J.-F., Lowe, J., et al.: The Scenario Model Intercomparison Project (ScenarioMIP) for CMIP6, *Geoscientific Model Development*, 9, 3461–3482, 2016.
- Pattyn, F., Ritz, C., Hanna, E., Asay-Davis, X., DeConto, R., Durand, G., Favier, L., Fettweis, X., Goelzer, H., Golledge, N. R., Kuipers Munneke, P., Lenaerts, J. T. M., Nowicki, S., Payne, A. K., Robinson, A., Seroussi, H., Trusel, L. D., and van den Broeke, M.: The Greenland and Antarctic ice sheets under 1.5 C global warming, *Nature Climate Change*, 8, 1053–1061, 2018.
- 445 Pavolonis, M. J. and Key, J. R.: Antarctic cloud radiative forcing at the surface estimated from the AVHRR Polar Pathfinder and ISCCP D1 datasets, 1985–93, *Journal of Applied Meteorology*, 42, 827–840, 2003.
- Scambos, T. A., Berthier, E., Haran, T., Shuman, C. A., Cook, A. J., Ligtenberg, S. R. M., and Bohlander, J.: Detailed ice loss pattern in the northern Antarctic Peninsula: widespread decline driven by ice front retreats, *The Cryosphere*, 8, 2135–2145, <https://doi.org/10.5194/tc-8-2135-2014>, 2014.
- 450 Scott, R. C., Nicolas, J. P., Bromwich, D. H., Norris, J. R., and Lubin, D.: Meteorological drivers and large-scale climate forcing of West Antarctic surface melt, *Journal of Climate*, 32, 665–684, 2019.
- Sherwood, S. C., Webb, M. J., Annan, J. D., Armour, K. C., Forster, P. M., Hargreaves, J. C., Hegerl, G., Klein, S. A., Marvel, K. D., Rohling, E. J., Watanabe, M., Andrews, T., Braconnot, P., Bretherton, C. S., Foster, G. L., Hausfather, Z., von der Heydt, A. S., Knutti, R., Mauritsen, T., Norris, J. R., Proistosescu, C., Rugenstein, M., Schmidt, G. A., Tokarska, K. B., and Zelinka, M. D.:
455 An Assessment of Earth’s Climate Sensitivity Using Multiple Lines of Evidence, *Reviews of Geophysics*, 58, e2019RG000678, <https://doi.org/https://doi.org/10.1029/2019RG000678>, 2020.
- Silber, I., Verlinde, J., Wang, S.-H., Bromwich, D. H., Fridlind, A. M., Cadetdu, M., Eloranta, E. W., and Flynn, C. J.: Cloud influence on ERA5 and AMPS surface downwelling longwave radiation biases in West Antarctica, *Journal of Climate*, 32, 7935–7949, 2019.
- Slingo, A.: A GCM parameterization for the shortwave radiative properties of water clouds, *Journal of the Atmospheric Sciences*, 46, 1419–
460 1427, 1989.
- Stephens, G. L.: The parameterization of radiation for numerical weather prediction and climate models, *Monthly Weather Review*, 112, 826–867, 1984.
- Sun, S., Cornford, S. L., Gwyther, D. E., Gladstone, R. M., Galton-Fenzi, B. K., Zhao, L., and Moore, J. C.: Impact of ocean forcing on the Aurora Basin in the 21st and 22nd centuries, *Annals of Glaciology*, 57, 79–86, 2016.
- 465 Trusel, L. D., Frey, K. E., Das, S. B., Munneke, P. K., and Van Den Broeke, M. R.: Satellite-based estimates of Antarctic surface meltwater fluxes, *Geophysical Research Letters*, 40, 6148–6153, 2013.
- Trusel, L. D., Frey, K. E., Das, S. B., Karnauskas, K. B., Kuipers Munneke, P., Van Meijgaard, E., and Van Den Broeke, M. R.: Divergent trajectories of Antarctic surface melt under two twenty-first-century climate scenarios, *Nature Geoscience*, 8, 927–932, 2015.



- 470 Van As, D., Van Den Broeke, M., Reijmer, C., and Van De Wal, R.: The summer surface energy balance of the high Antarctic plateau, *Boundary-Layer Meteorology*, 115, 289–317, 2005.
- van den Broeke, M.: Strong surface melting preceded collapse of Antarctic Peninsula ice shelf, *Geophysical Research Letters*, 32, 2005.
- Van Den Broeke, M., Reijmer, C., Van As, D., and Boot, W.: Daily cycle of the surface energy balance in Antarctica and the influence of clouds, *International Journal of Climatology: A Journal of the Royal Meteorological Society*, 26, 1587–1605, 2006.
- 475 Van Wessem, J. M., Jan Van De Berg, W., Noël, B. P., Van Meijgaard, E., Amory, C., Birnbaum, G., Jakobs, C. L., Krüger, K., Lenaerts, J., Lhermitte, S., et al.: Modelling the climate and surface mass balance of polar ice sheets using racmo2: Part 2: Antarctica (1979-2016), *Cryosphere*, 12, 1479–1498, 2018.
- Wang, C., Soden, B. J., Yang, W., and Vecchi, G. A.: Compensation Between Cloud Feedback and Aerosol-Cloud Interaction in CMIP6 Models, *Geophysical Research Letters*, 48, e2020GL091 024, 2021.
- 480 Wang, W., Zender, C. S., van As, D., and Miller, N. B.: Spatial distribution of melt season cloud radiative effects over Greenland: Evaluating satellite observations, reanalyses, and model simulations against in situ measurements, *Journal of Geophysical Research: Atmospheres*, 124, 57–71, 2019.
- Wille, J. D., Favier, V., Dufour, A., Gorodetskaya, I. V., Turner, J., Agosta, C., and Codron, F.: West Antarctic surface melt triggered by atmospheric rivers, *Nature Geoscience*, 12, 911–916, 2019.
- 485 Wyser, K., Noije, T. v., Yang, S., Hardenberg, J. v., O'Donnell, D., and Döscher, R.: On the increased climate sensitivity in the EC-Earth model from CMIP5 to CMIP6, *Geoscientific Model Development*, 13, 3465–3474, 2020.
- Zelinka, M. D., Myers, T. A., McCoy, D. T., Po-Chedley, S., Caldwell, P. M., Ceppi, P., Klein, S. A., and Taylor, K. E.: Causes of higher climate sensitivity in CMIP6 models, *Geophysical Research Letters*, 47, e2019GL085 782, 2020.
- Zhang, T., Starnes, K., and Bowling, S.: Impact of clouds on surface radiative fluxes and snowmelt in the Arctic and subarctic, *Journal of Climate*, 9, 2110–2123, 1996.
- 490 Zhu, J., Poulsen, C. J., and Otto-Bliesner, B. L.: High climate sensitivity in CMIP6 model not supported by paleoclimate, *Nature Climate Change*, 10, 378–379, 2020.